The HKU Scholars Hub   The University of Hong Kong   香港大學學術庫

Title	Eigen-based clutter filters for color flow imaging: Single-ensemble vs. multi-ensemble approaches
Author(s)	Yu, ACH; Løvstakken, L
Citation	The 2007 IEEE Ultrasonics Symposium, New York, N.Y., 28-31 October 2007. In Conference Proceedings of IEEE Ultrasonics Symposium, 2007, p. 1101-1104
Issued Date	2007
URL	http://hdl.handle.net/10722/99764
Rights	IEEE International Ultrasonics Symposium Proceedings. Copyright © IEEE.

Eigen-Based Clutter Filters for Color Flow Imaging: Single-Ensemble vs. Multi-Ensemble Approaches

Alfred C. H. Yu* and Lasse Løvstakken†

*Dept. of Electrical and Electronic Engineering, The University of Hong Kong, Pokfulam, Hong Kong SAR
†Dept. of Circulation and Medical Imaging, The Norwegian University of Science and Technology, Trondheim, Norway

Correspondance Emails: alfred.yu@eee.hku.hk, lasse.lovstakken@ntnu.no

Abstract—In designing eigen-based clutter filters for color flow imaging, one of the challenges is to develop an accurate way of estimating the eigen-components that represent clutter in slow-time ensembles. To provide new insights on the problem, this paper presents a comparative analysis on how eigen-filters perform when using eigen-estimation methods that involve multiple ensembles or a single ensemble. The analysis consists of two parts: 1) a comparative review on the principles behind different eigen-estimation methods; 2) an eigen-filtering experiment done with coronary flow imaging data acquired from a porcine during bypass graft operation. For an imaging case containing tissue motion due to myocardial contraction, our analysis showed that the single-ensemble eigen-filter shared similar performance with a multi-ensemble eigen-filter that uses small (5x5) ensemble windows (with about 1 dB difference in clutter suppression level). Results also showed that a multi-ensemble eigen-filter with large (20x20) ensemble windows yielded poorer performance (clutter suppression level was 3 to 6 dB lower).

Index Terms—color flow imaging, clutter supression, eigen-based filters, eigen-component estimation.

I. INTRODUCTION

An important step in the processing of color flow imaging data is the suppression of slow-time clutter originating from tissue reverberations and beam sidelobe leakages. If done properly, this clutter filtering step can reduce the amount of flashing or blooming artifacts seen in color flow images. Over the past decade, various clutter filtering solutions have been developed in attempt to improve the visualization performance of color flow images [1]. Amongst the solutions reported, the eigen-based filter has been suggested to have potential in adaptively suppressing slow-time clutter with variable spectral characteristics. This filter works by directly removing eigen-components (or orthogonal bases) that represent clutter in the slow-time signal [2]–[7]. Its attenuation response is in theory adapted to the clutter contents because the eigen-components are estimated based on the actual slow-time signal statistics. Nevertheless, its practical efficacy in color flow data processing has not been well-established because there are two design issues that have not been properly addressed: 1) the estimation approach used to determine the eigen-components, and 2) the algorithm used to identify the eigen-components that are related to clutter. As such, further investigations are still needed to fine-tune the formulation of the eigen-based

filter and to demonstrate its effectiveness in suppressing slow-time clutter.

The aim of this work is to acquire a better understanding of one specific eigen-filter design issue: the methodology used to estimate the eigen-components of a slow-time ensemble. In particular, it is our intent to comparatively assess the performance of eigen-component estimation methods that involve either multiple slow-time ensembles [2]–[6] or only a single slow-time ensemble [7]. In the next section, we shall review and compare the theoretical principles behind these two eigen-estimation approaches. We will then present an in-vivo imaging example that demonstrates how the two eigen-estimation approaches perform in eigen-based clutter filtering.

II. THEORY

A. Basic Principles of Eigen-Based Clutter Filters

A conceptual illustration of the eigen-based filter is shown in Fig. 1. This filtering strategy generally begins by decomposing a sample volume's slow-time signal contents into a sum of mutually orthogonal components that have the minimum mean-squared modeling error [2]–[7]. Such a signal decomposition, often referred to as the Karhunen-Loeve expansion, can be mathematically expressed as follows for a given slow-time ensemble vector $\mathbf{x}$ with N_D samples:

$$\mathbf{x} = [x(0), x(1), \ldots, x(N_D - 1)]^T = \sum_k \gamma_k \mathbf{e}_k. \quad (1)$$

In the above, $\mathbf{e}_k$ is the kth eigenvector (of length N_D), while γ_k is the corresponding expansion weight that satisfies the following orthogonality relation:

$$E\left\{ (\gamma_k \mathbf{e}_k)^{*T} (\gamma_l \mathbf{e}_l) \right\} = \left\{ \begin{array}{ll} \lambda_k & (k = l) \\ 0 & (k \neq l) \end{array} \right. , \quad (2)$$

where λ_k is referred to as the kth eigenvalue. By definition, the eigen-components in (1) are ordered in a descending energy order, and hence $\lambda_k \mathbf{e}_k$ can be considered as the kth principal eigen-component. The goal of the eigen-based filter is to then identify the eigen-components that represent clutter in the slow-time signal. Assuming that the K_c largest eigen-components correspond to clutter, the filtered slow-time ensemble $\mathbf{y}$ is simply equal to the following matrix product
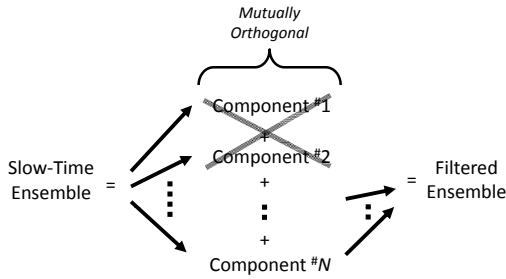
Fig. 1. Conceptual illustration of the principles behind eigen-based clutter filters. During the filtering process, eigen-components (often the more dominant ones) that represent clutter are removed.
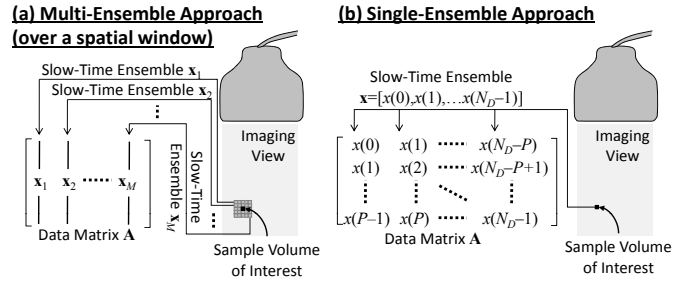

Fig. 2. Principles of two different eigen-component estimation methods: (a) a multi-ensemble approach that uses a set of slow-time ensembles within a spatial window; (b) a single-ensemble approach that involves redundant use of slow-time data samples.

between the raw ensemble and the orthogonal projection of all the clutter eigenvectors:

$$\mathbf{y} = (\mathbf{I} - \mathbf{CC}^{\dagger})\mathbf{x}, \quad \mathbf{C} = \begin{bmatrix} | & | & & | \\ \mathbf{e}_1 & \mathbf{e}_2 & \cdots & \mathbf{e}_M \\ | & | & & | \end{bmatrix}, \quad (3)$$

where the '$\dagger$' superscript denotes a pseudoinverse operation (i.e. the singular matrix version of matrix inverses). Note that K_c can be interpreted as the $(K_c - 1)^{th}$ eigen-filter order.

B. Overview of Eigen-Component Computation

The common way of finding the eigen-components in (1) is to compute the eigenvalue decomposition (EVD) of the slow-time signal's correlation matrix (i.e. $E\{\mathbf{xx}^{*T}\}$, or the expected outer product between the signal vector and its conjugate transpose). This computation approach stems from matrix algebra's version of the spectral theorem [8], which relates the slow-time correlation matrix $\mathbf{R}$ to the eigen-components in (1) as follows based on the orthogonality principle:

$$\mathbf{R} = E\{\mathbf{xx}^{*T}\} = \sum_k \lambda_k \mathbf{e}_k \mathbf{e}_k^{*T}. \quad (4)$$

Since the correlation matrix in (4) has a self-adjoint structure (i.e. $\mathbf{R} = \mathbf{R}^{*T}$), it is possible to define a non-square data matrix $\mathbf{A}$ that satisfies the relation $\mathbf{R} = \mathbf{AA}^{*T}$. It follows that the singular value decomposition (SVD) of $\mathbf{A}$ is connected to the EVD of $\mathbf{R}$ according to the following duality relation:

$$\mathbf{A} = \sum_k \sigma_k \mathbf{u}_k \mathbf{v}_k^{*T} \iff \mathbf{AA}^{*T} = \sum_k \sigma_k^2 \mathbf{u}_k \mathbf{u}_k^{*T} \equiv \mathbf{R}, \quad (5)$$

where σ_k is the kth singular value with $\mathbf{u}_k$ and $\mathbf{v}_k$ as the corresponding left/right singular vectors. Comparing between (4) and (5), it can be seen that: 1) the eigenvectors in the EVD of $\mathbf{R}$ are equivalent to the left singular vectors in the SVD of $\mathbf{A}$, and 2) each eigenvalue is essentially the square of the corresponding singular value. These two properties show that both the SVD of $\mathbf{A}$ and the EVD of $\mathbf{R}$ may be used to calculate the eigen-components in (1). Note that EVD/SVD can be solved using numerical algorithms such as power iterations and QR factorization [8].

To carry out the above eigen-computation approaches in practice, it is necessary to first estimate the slow-time correlation matrix $\mathbf{R}$ or the data matrix $\mathbf{A}$. As reported in

existing eigen-filter designs, this estimation process can be done based on formulations that involve either multiple slow-time ensembles or a single slow-time ensemble. The principles of both formulations and their suitability in slow-time clutter filtering will be discussed in the following subsections.

C. Eigen-Estimation Based on Multiple Ensembles

One method of estimating the slow-time correlation matrix during operations is to first create a data matrix by stacking together multiple realizations of slow-time ensembles (see Fig. 2a) and then compute the outer product between the data matrix and its conjugated transpose. For a set of M slow-time ensembles, this formulation would give the following forms of the data matrix $\mathbf{A}$ (with size $N_D \times M$) [2] and the correlation matrix $\mathbf{R}$ (with size $N_D \times N_D$) [3]–[6]:

$$\mathbf{A} = \frac{1}{\sqrt{M}} \begin{bmatrix} | & | & & | \\ \mathbf{x}_1 & \mathbf{x}_2 & \cdots & \mathbf{x}_M \\ | & | & & | \end{bmatrix}, \quad (6)$$

$$\mathbf{R} = \mathbf{AA}^{*T} = \frac{1}{M} \sum_{m=1}^{M} \mathbf{x}_m \mathbf{x}_m^{*T}, \quad (7)$$

where $\mathbf{x}_m$ is the mth realization in the ensemble set. Note that the SVD/EVD computed from these two matrices would comprise N_D eigen-components if (6) and (7) have full matrix rank (i.e. linear independence between all rows), which can be achieved when the number of slow-time ensembles is at least equal to the ensemble size (i.e. $M \geq N_D$). Nevertheless, the ensemble set used to form (6) and (7) is required to possess similar clutter statistics because these matrices are formed via ensemble stacking and averaging. In the literature, it was suggested that the ensemble set can be chosen either from sample volumes along the same beam line [2]–[5] or from ones within a spatial window centered about the sample volume concerned [6]. The latter way, which is illustrated in Fig. 2a, seems more appropriate since adjacent sample volumes within an imaging view are more likely to share similar clutter statistics.

D. Eigen-Estimation Based on a Single Ensemble

Instead of relying on multiple ensembles, it is possible to use a single slow-time ensemble to form the matrices $\mathbf{A}$ and

R. In this second formulation, the slow-time data matrix is created by dividing a slow-time ensemble into lag-one overlapping subsets and stacking the subsets together in different columns (see Fig. 2b). The resulting data matrix would take on the following Hankel structure (i.e. with constant reverse diagonals) [7]:

$$\mathbf{A} = \frac{1}{\sqrt{P}} \begin{bmatrix} x(0) & x(1) & \cdots & x(N_D - P) \\ x(1) & x(2) & \cdots & x(N_D - P + 1) \\ \vdots & \vdots & \ddots & \vdots \\ x(P-1) & x(P) & \cdots & x(N_D - 1) \end{bmatrix},$$

(8)

where P is a dimension parameter representing the subset size and it is often set to `ceil`$(N_D/2)$ to form the most subsets from a slow-time ensemble. From the $P \times (N_D - P + 1)$ data matrix defined in (8), a slow-time correlation matrix of size $P \times P$ can then be computed as:

$$\mathbf{R} = \mathbf{A}\mathbf{A}^{*T}$$
$$= \begin{bmatrix} R_0(0) & R_1(-1) & \cdots & R_{P-1}(-P+1) \\ R_0(1) & R_1(0) & \cdots & R_{P-1}(-P+2) \\ \vdots & \vdots & \ddots & \vdots \\ R_0(P-1) & R_1(P-2) & \cdots & R_{P-1}(0) \end{bmatrix},$$

(9)

with $R_k(l)$ being the lth-lag autocorrelation estimate found from the following average of correlation values over an ensemble subset of $N_D - P + 1$ samples (with k as the first sample index at lag-zero):

$$R_k(l) = \frac{1}{P} \sum_{n=k+l}^{N_D - P + k + l} x(n)x^*(n-l).$$

(10)

Note that (8) and (9) theoretically assumes statistical stationarity between samples in the slow-time ensemble because of the data redundancy introduced in the matrix structures. Also, their respective SVD/EVD would give P eigen-components with size-P vectors. Since $P = $ `ceil`$(N_D/2)$ in most cases, as mentioned above, the maximum number and size of eigen-components obtainable from this eigen-estimation method are both equal to `ceil`$(N_D/2)$, or half the amount available from the multi-ensemble formulation. To reconstruct eigen-components with size-N_D vectors as needed for the filtering in (3), we can first create a rank-one Hankel matrix from each singular vector pair's outer product $\mathbf{u}_k\mathbf{v}_k^{*T}$ and then average along the N_D reverse diagonals of this matrix [7].

III. EXPERIMENTAL WORK

A. Overview of Study

To assess the impact of different eigen-estimation methods on the performance of eigen-filters, we conducted a clutter filtering experiment using intra-operative flow imaging data acquired from a pig's coronary anastomosis during a bypass graft operation. Table I lists the data acquisition parameters used in this study, and Fig. 3a (next page) shows a B-mode image of the field-of-view. It is worth noting that the

TABLE I
EXPERIMENTAL PARAMETERS

Parameter	Value
Transmit pulse frequency	10 MHz
Pulse repetition frequency	2.5 kHz
Slow-time ensemble size	10
Beam line interleaving ratio	13 to 1
Lateral field of view	-7.8 to +7.8 mm (182 beam lines)
Axial field of view	0 to +15 mm (195 depth sections)

TABLE II
CLUTTER SUPPRESSION LEVEL (DECIBEL SCALE) IN TISSUE REGIONS

Eigen-Filter Type	EPICARDIUM	BELOW ANASTOMOSIS
5×5 Multi-Ensemble	21.6	48.7
20×20 Multi-Ensemble	18.9	43.9
Single-Ensemble	22.7	49.9

dataset was acquired in the presence of apparent tissue motion originating from cardiac contraction. As such, the imaging data contains clutter with spatially and temporally varying features.

B. Analysis Procedure

In this work, we evaluated eigen-based clutter filters that make use of three different eigen-estimation strategies: 1) the single-ensemble approach; 2) the multi-ensemble approach based on 5×5 ensemble windows (0.39×0.43 mm^2); 3) another one based on 20×20 ensemble windows (1.54×1.71 mm^2). Each form of eigen-filter was applied to the raw slow-time ensemble of every sample volume within the imaging view, and the filtered signal power estimates were used to produce Doppler power maps. During the eigen-filtering process, the K_c clutter eigen-components were identified by finding the dominant eigen-components with mean frequency (estimated via the lag-one autocorrelator) inside a prescribed clutter band centered at the mean frequency of the most dominant eigen-component. This frequency-based filter order selection algorithm was used because it can more robustly identify clutter eigen-components than other algorithms [9]. Note that the clutter band was empirically chosen to be 250 Hz (0.1 norm freq) in our imaging example since it gave the most consistent visualization of the blood vessels.

C. Results

Figs. 3b through 3d show the Doppler power maps obtained from the three forms of eigen-based filters being tested. Also, Table II summarizes the clutter suppression level (i.e. average power removed) in different tissue regions. Two observations should be noted from these results. First, the single-ensemble eigen-filter seems to share similar performance with the 5×5 multi-ensemble eigen-filter (with about 1 dB difference in clutter suppression level). Second, smearing artifacts can be seen in the power image obtained from the multi-ensemble eigen-filter that uses 20×20 ensemble windows, suggesting that this filter is less capable of suppressing slow-time clutter. Indeed, its clutter suppression level was between 3 to 6 dB worse than the other two eigen-filters.
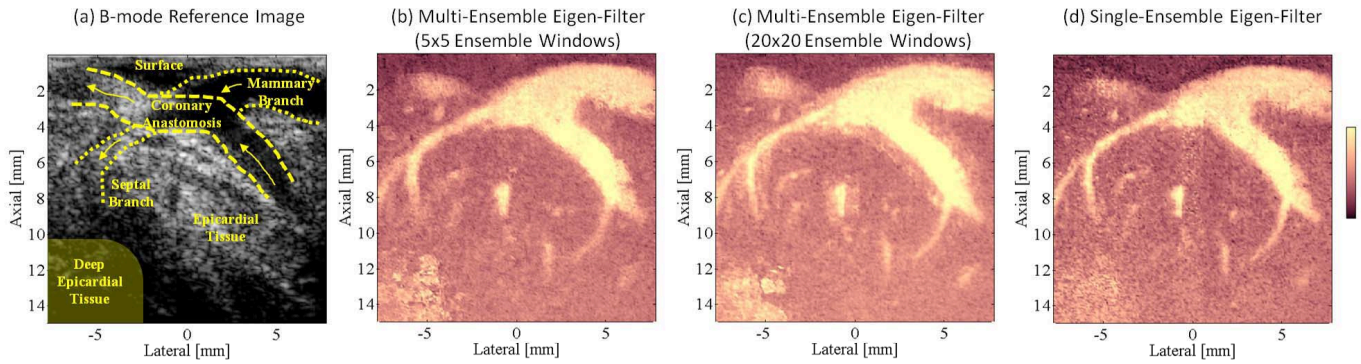
Fig. 3. Results for the eigen-filtering experiment. Part (a) shows the B-mode image of the field of view. Marked in yellow are the contours of coronary graft, epicardial tissues, and other arterial branches. Parts (b), (c), and (d) show the Doppler power maps obtained respectively from the 5×5 multi-ensemble eigen-filter, the 20×20 multi-ensemble eigen-filter, and the single-ensemble eigen-filter. The dynamic range of the power map scale is 40 dB. The analysis procedure used was described in Sec. III-B.

IV. DISCUSSION

A. Efficacy of Multi-Ensemble Eigen-Estimation Method

In our imaging example, the 5×5 multi-ensemble eigen-filter showed better clutter suppression performance than the one that uses 20×20 ensemble windows (improvements of roughly 3 dB in epicardium and 5 dB near anastomosis). This finding suggests that, for eigen-filters involving the multi-ensemble eigen-estimation method, the use of a smaller ensemble window (0.39×0.43 mm^2 in our case) seems more suitable than a larger one (1.54×1.71 mm^2). Such a deduction can be explained by considering the multi-ensemble approach's statistical stationarity assumption, which expects all the slow-time ensembles in the window to share similar clutter statistics (because **A** and **R** are formed via ensemble stacking and averaging). Given this statistical assumption, the multi-ensemble approach is more likely to give accurate estimates of the clutter eigen-components (and hence lead to effective clutter filtering) when using smaller ensemble windows over which tissue motion is more likely to remain coherent. Conversely, the approach may give rise to leakages in the clutter eigen-components (and hence reduced clutter filtering efficacy) when using larger ensemble windows that may have incoherent tissue motion within. This latter explanation may indeed be the prime reason for why smearing artifacts are seen in the Doppler power map of the 20×20 multi-ensemble eigen-filter.

B. Efficacy of Single-Ensemble Eigen-Estimation Method

Another key result shown in our imaging example is that the single-ensemble eigen-filter seems capable of suppressing clutter in the tissue regions, particularly the ones in the deep epicardium. This finding is in agreement with the previous subsection's conclusion that smaller ensemble windows lead to better clutter suppression performance (the window size is simply 1×1 for the single-ensemble approach). Though from a theoretical angle, such a finding may seem surprising because the single-ensemble approach's stationarity assumption in slow-time inherently forces the eigen-components to

be complex sinusoids that are less representative of non-sinusoidal clutter arising from accelerative tissue motion. A likely reason for not suffering much performance drops due to this theoretical limitation is that the slow-time spectral resolution may be too low (PRF/N_D=250 Hz in our case) for accelerative tissue's clutter to be necessarily treated as non-sinusoids. Nevertheless, the impact of the slow-time stationarity assumption may become more prominent when the slow-time spectral resolution is improved (e.g. through lowering the pulse repetition frequency or acquiring more data samples).

REFERENCES

[1] A. C. H. Yu, K. W. Johnston, and R. S. C. Cobbold, "Frequency-based signal processing in ultrasound color flow imaging," *Can. Acoust.*, vol. 35(2), pp. 11–23, 2007.
[2] L. A. F. Ledoux, P. J. Brands, and A. P. G. Hoeks, "Reduction of the clutter component in doppler ultrasound signals based on singular value decomposition: a simulation study," *Ultrason. Imaging*, vol. 19, pp. 1–18, 1997.
[3] C. M. Gallippi and G. E. Trahey, "Adaptive clutter filtering via blind source separation for two-dimensional ultrasonic blood velocity measurement," *Ultrason. Imaging*, vol. 24, pp. 193–214, 2002.
[4] S. Bjærum, H. Torp, and K. Kristoffersen, "Clutter filters adapted to tissue motion in ultrasound color flow imaging," *IEEE Trans. Ultrason. Ferroelec. Freq. Contr.*, vol. 49, pp. 693–704, 2002.
[5] C. Kargel, G. Hobenreich, B. Trummer, and M. F. Insana, "Adaptive clutter rejection filtering in ultrasonic strain-flow imaging," *IEEE Trans. Ultrason. Ferroelec. Freq. Contr.*, vol. 50, pp. 824–835, 2003.
[6] L. Løvstakken, S. Bjærum, K. Kristoffersen, R. Haaverstad, and H. Torp, "Real-time adaptive clutter rejection filtering in color flow imaging using power method iterations," *IEEE Trans. Ultrason. Ferroelec. Freq. Contr.*, vol. 53, pp. 1597–1608, 2006.
[7] A. C. H. Yu and R. S. C. Cobbold, "A new eigen-based clutter filter using the Hankel-SVD approach," *Proc. IEEE Ultrason. Symp.*, pp. 1079–1082, 2006.
[8] T. K. Moon and W. C. Stirling, *Mathematical Methods and Algorithms for Signal Processing*, ch. 6 & 7. Prentice Hall Inc., 2000.
[9] L. Løvstakken, A. C. H. Yu, and H. Torp, "In-vivo investigation of filter order influence in eigen-based clutter filtering for color flow imaging," *Proc. IEEE Ultrason. Symp.*, no. P6B-3, 2007.